Development of Novel EBSM System for High-Tech Material Additive Manufacturing Research

C. Guo[1, 2, 3], F. Lin[1, 2, 3], W. J. Ge[1, 2, 3] and J. Zhang[1, 2, 3]

1. Department of Mechanical Engineering, Tsinghua University, Beijing 100084;
2. Key Laboratory for Advanced Materials Processing Technology, Ministry of Education of China, Tsinghua University, Beijing 100084;
3. Biomanufacturing and Rapid Forming Technology Key Laboratory of Beijing, Tsinghua University, Beijing 100084.

REVIEWED

Abstract

Electron beam is more appropriate for metal additive manufacturing (AM) than laser because of its high energy converting efficiency and high absorption for various materials. It becomes a preference for AM study of high-tech material with high melting point, high brittleness or graded material. A novel electron beam selective melting (EBSM) system with dual-material processing capability has been developed in Tsinghua University to meet the wide high-tech material AM research requirement. A vibration driven powder supplier was developed and the supplier had a high compatibility to various powders. A stable supplying rate and a supplying accuracy less than 7.5% were obtained with the supplier. Two powders can be supplied individually to obtain a mixture with tailored proportion for each powder layer. The mixture is homogenous and the actual proportion is close to the desired value. In order to prolong the spreading comb's lifetime and avoid tooth breaking, a low deformation powder spreading device was designed based on dual inclined combs and a one-way scraping mechanism. The system provides exchangeable building tanks with sizes of 100 × 100 × 100 mm^3 and 250 × 250 × 250 mm^3, which can save powder when the part is small and the powder is expensive. The novel EBSM system is capable of building parts with single material and has a potential of dual-material processing.

1. Introduction

Electron Beam Selective Melting (EBSM) is an additive manufacturing technique that builds metal parts layer by layer by using an electron beam to selectively scan and melt the powder layer in a vacuum chamber. Compared to the laser process such as Selective Laser Sintering/Melting (SLS/SLM), EBSM has some features. First, the converting efficiency from electric energy to electron beam energy and the absorptivity of electron beam for metal powder are high. As a result, the electron beam can produce highly dense parts with high melting point materials, e.g. Ti-6Al-4V. Second, before melting the cross-section of the part, the electron beam preheats the powder bed to a high temperature with a fast scanning velocity. The preheat step not only slightly sinters the powder so as to avoid the collapse of the lowly conductive powder bed,

but also plays a role as the heat treatment, thus efficiently reduces the thermal stress during fabrication and decreases the brittleness of the fabricated parts. Therefore, EBSM is appropriate for manufacturing parts with high brittleness materials, e.g. TiAl alloy. With the above advantages, EBSM was attracting more and more attentions these years and is regarded as a preferential additive manufacturing technique for high-tech metal.

Currently, the corporation ARCAM AB has developed several commercial EBSM machines which are increasingly used in medical implant and aerospace industries. Parts with various materials has been successfully manufactured via EBSM, e. g. 316L stainless steel, Ti alloy, Co-based alloy, Ni-based superalloy, TiAl alloy [1-5]. However, the application of EBSM still needs to be further expanded so that the overall potential of EBSM can be used to its full capacity. One of the possible new applications of EBSM is the manufacturing of graded materials. Some researchers investigated the feasibility of multi-material processing of SLM. Liu, et al. fabricated 316L stainless steel and UNS C18400 Cu alloy dual-material samples with SLM: after depositing many layers of 316L stainless steel, Cu alloy was sequentially deposited on the previous layers. The interfacial characterization of the samples was investigated and it is found that cracks occasionally appear on the interface [6]. Terrazas, et al. fabricated multi-material structures using Ti-6Al-4V and copper powder with the EBSM technology. The fabricated part with the first material was machined to provide a surface on which the second material was deposited [7]. However, the process can not be completed in a single machine run and the interfacial region was narrow, which would affect the performance of the graded material.

In addition, the materials for EBSM need further expansion and it calls for a wide material compatibility of the EBSM system. Especially in the material study, the EBSM system is expected to fabricate samples with various materials with various particle shapes and various particle sizes. EBSM system with wide material compatibility would help the researchers to study new material, optimize the process, and get deep insight into the EBSM technology.

In this paper, a novel EBSM system with a capacity of dual-materials processing and with a wide material compatibility was developed. A vibration driven powder supplier was designed. Two different powders can be supplied individually and precisely and then mixed. The mixing ratio of each powder layer can be tailored so that parts with material in gradual change can be fabricated. In order to prolong the spreading comb's lifetime and avoid breaking of the comb tooth, a low deformation powder spreading device with dual inclined combs and a one-way scraping mechanism were designed. The new EBSM system provides two exchangeable building tanks with sizes of $100 \times 100 \times 100$ mm^3 and $200 \times 200 \times 200$ mm^3, which can save powder when the part is small and the powder is expensive. Some experiments and their results are presented in this paper.

2. Description of the System

2.1. Vibration Driven Powder Supplier and the Powder Mixer

Fig. 1 is a schematic of the vibration driven powder supplier. A vibration plate is placed at the lower opening of the powder storage, and the space between the vibration plate and the baffle board provides the powder an exit. While the vibrator stops vibrating, the powder forms a repose angle due to internal friction. While the vibrator starts working, the vibration plate moves back

and forth at a high frequency. As a result, the powder continuously moves on the vibration plate, generating a stable powder flow off the vibration plate. The powder supplier driven by vibration has no rotatable parts, thus has high reliability in the dust environment.

Fig. 2 is a schematic of the dual powders mixer. Two powder suppliers are placed side by side, facing each other. A powder mixing box is placed right below the edges of the vibration plates, and a weight senor is used to measure the weight of powder in the mixing box in real time. Once the powder weight reaches the desired value, the vibrator stops working. The two powders can be supplied into the mixing box individually and precisely to obtain a mixture with desired proportion. Then, the mixing box rotates back and forth, blends the two powders, and finally pours the mixture onto the working platform.

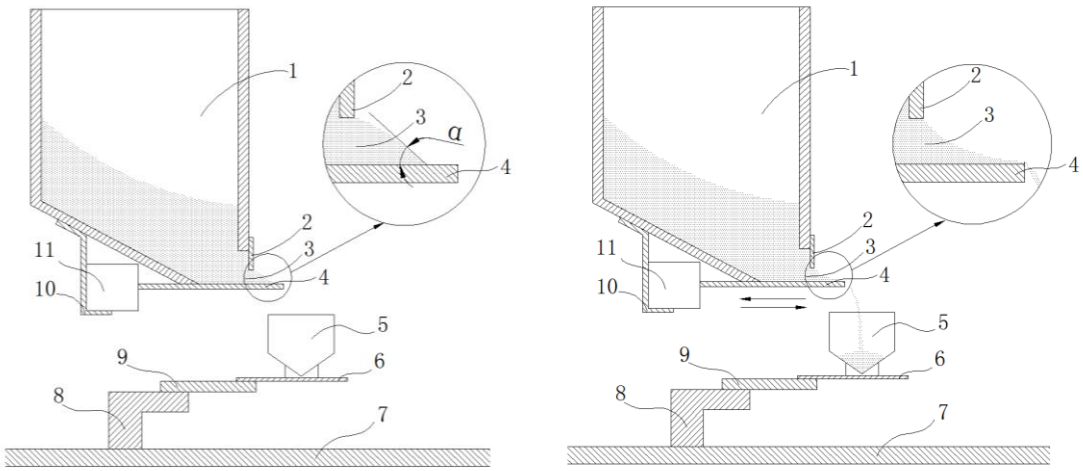

(a) Stop vibrating (b) Vibrating

Fig.1. Schematic of the vibration driven powder supplier

1, powder storage; 2, baffle board; 3, powder exit; 4, vibration plate; 5, mixing box; 7, working platform; 8, supporting block; 9, weight sensor; 10, connection; 11, Vibrator.

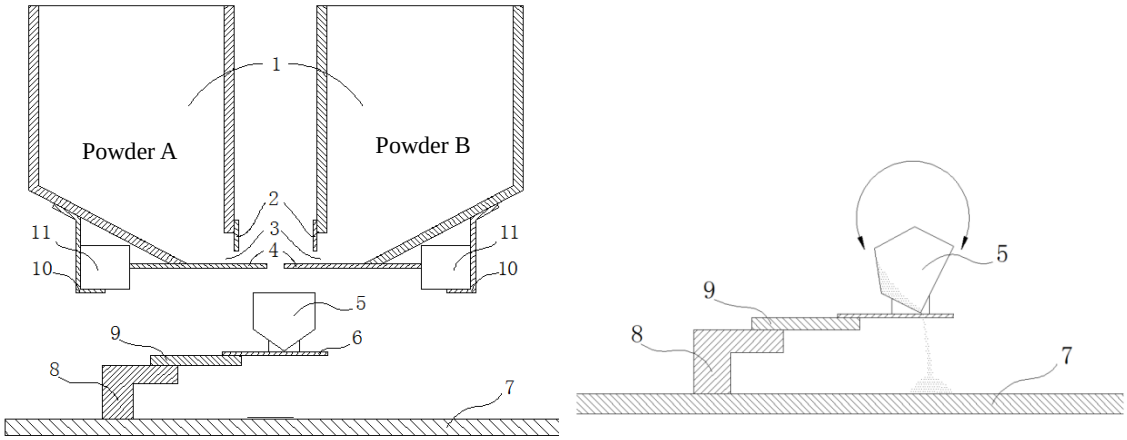

(a) Dual powder supplier (b) Powder mixing

Fig.2. Schematic of the dual powders mixer

1, powder storage; 2, baffle board; 3, powder exit; 4, vibration plate; 5, mixing box; 7, working platform; 8, supporting block; 9, weight sensor; 10, connection; 11, Vibrator.

2.2. Low Deformation Powder Spreading Device

During the EBSM, balling phenomena often occur, resulting in bumps on the deposited surface. On this occasion, the powder spreader needs to scrap over the bump, leading to the bending of the comb teeth. Vertical combs are commonly used in the additive manufacturing technologies based on powder bed. Unfortunately, permanent deformation or breaking of the comb teeth often occurs. The picture in Fig. 3 shows an example of the permanent deformation of the comb teeth. After scraping over the balling surface several times, irrecoverable deformation is found in some of the comb teeth. The deformed comb leads to an uneven surface of the powder bed, and worsens the fabrication quality in the following deposition. In this study, instead of the vertical comb, the inclined comb is utilized so as to reduce the risk of teeth deformation or breaking.

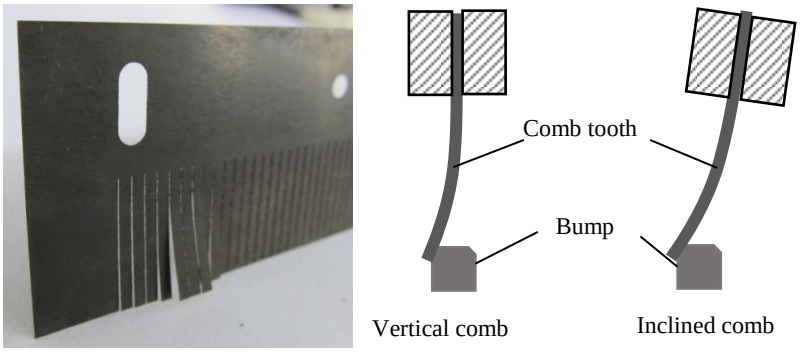

Fig. 3. Vertical and inclined comb

In order to enhance the reliability of spreading device, a dual-combs design is adopted in the EBSM system. Two parallel combs are placed in tandem, the front comb keeps off the working platform a small distance, while the back one is exactly on the working platform. In addition, one comb is offset half of teeth width relative to the other comb. As a result, powder leaked between the teeth of the front comb can be leveled down by the back comb.

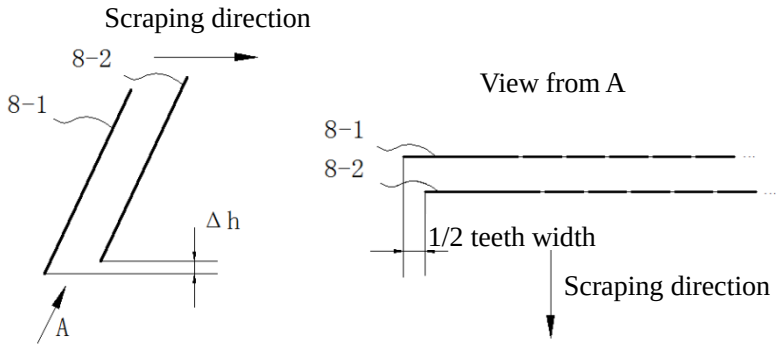

Fig. 4. Dual inclined combs

As shown in Fig. 4, since the comb is inclined, the comb should move towards the inclined direction. If the comb moves in the opposite direction, the comb teeth have high risk of getting stuck on the uneven deposited surface. Therefore, a one-way scraping mechanism as shown in Fig. 5 is designed. As illustrated in Fig. 5a, by twisting the adjusting screw, the wheel is constrained on the lower surface of the guide rail. As the slide moves forwards, the combs scraps on the working platform and spreads the powder into the building tank. As the slide moves to the end, the wheel rises along the wedge block, lifts the bridge plate, and then moves onto the upper

surface of the guide rail (see in Fig. 5b). Consequently, as the slide moves backwards, the combs returns back to the original position, without contacting with the working platform (see in Fig. 5c).

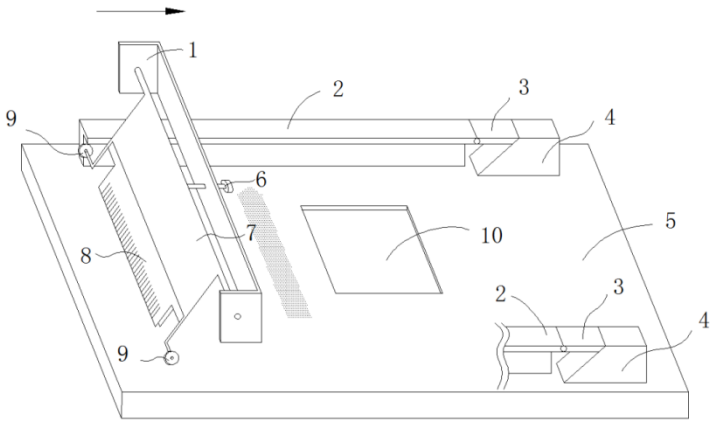

(a) Original position

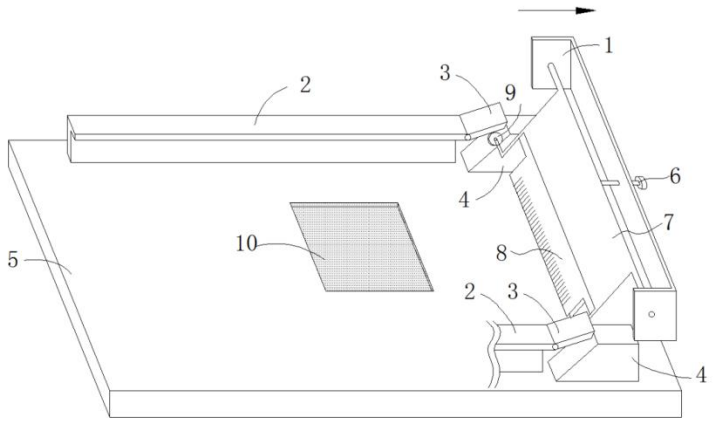

(b) Moving forwards

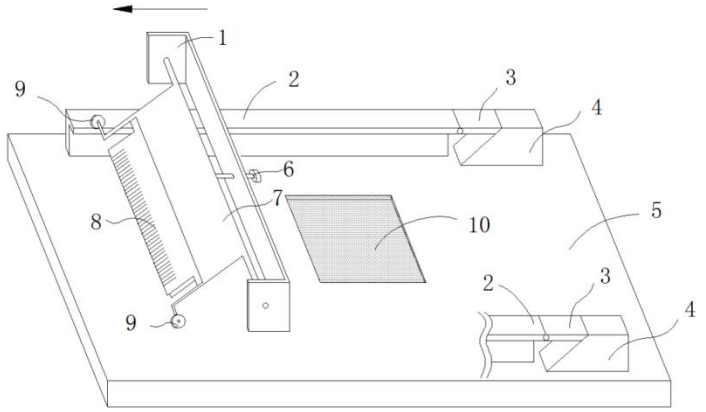

(c) Moving backwards

Fig. 5. Schematic of the one-way scraping mechanism

1, slider; 2, guide rail; 3, bridge plate; 4, wedge block; 5, working platform; 6, adjusting screw; 7, mounting plate; 8, combs; 9, wheel; 10, building tank.

2.3. Exchangeable Building Tanks with Different Sizes

The EBSM system provides two exchangeable building tanks with sizes of 100 × 100 × 100 mm^3 and 250 × 250 × 250 mm^3. As illustrated in Fig. 6, if the part needs to be fabricated is small and the powder is expensive, the larger building tank can be replaced by the smaller one to reduce the material cost.

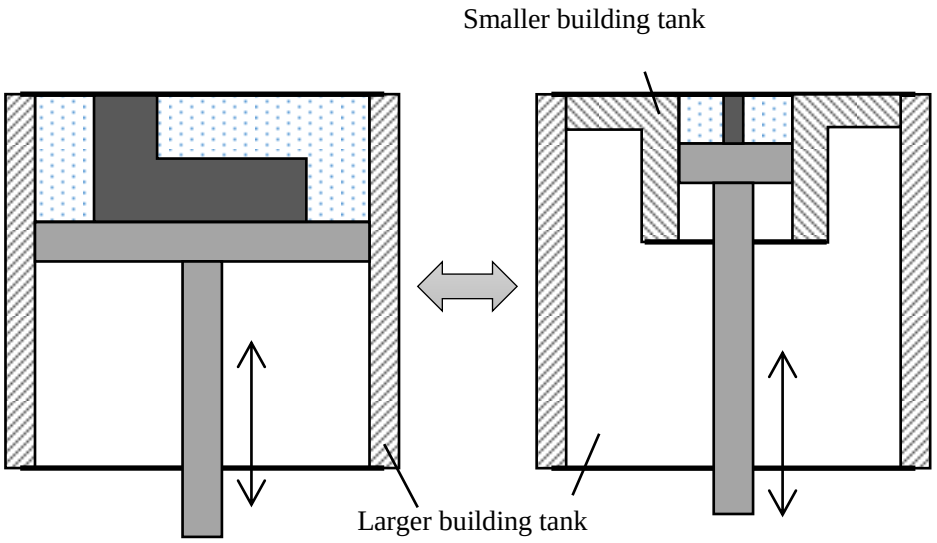

Fig. 6. Exchangeable building tanks

3. Experiments and Results

3.1. Material Compatibility of the Supplier

Various powders including sponge Ti, gas and water atomized 316L stainless steel and gas atomized Ti-6Al-4V were tested on the powder supplier. For these 6 kinds of powders, the powder supplying was continuous and stable, and their supplying rates were listed in Table 1. The powder supplier has a high compatibility to different powders. The supplying rate increases with the increase of powder flowability. The 300 mesh sponge Ti powder has the lowest flowability, thus its supplying rate is the lowest. The 100 mesh gas atomized 316L stainless steel powder has the highest flowability, and thus has a fastest supplying rate. Among the gas atomized 316L stainless steel powders, the supplying rate increases with the decrease of mesh number. In other words, a larger powder particle size leads to a higher flowability and supplying rate. Another issue influencing the supplying rate is the powder exit size. A larger exit size leads to a higher supplying rate. For powder with higher flowability, the powder exit size should be reduced to obtain the same supplying rate.

The errors between the desired and actual weight in powder supplying were measured using the 200 mesh gas atomized 316L stainless steel powder, and the results were presented in Fig. 7. The actual weight of powder fluctuates near the desired value, and the maximum error is 7.5%.

Table 1. Powder supplying rates (g/s) for various powders

Powder exit size (Wide ×Height)	300 mesh sponge Ti	200 mesh water atomized 316L stainless steel	300 mesh gas atomized 316L stainless steel	200 mesh gas atomized Ti-6Al-4V	200 mesh gas atomized 316L stainless steel	100 mesh gas atomized 316L stainless steel
60 ×1	--	--	--	--	--	1.69
60 ×2	--	--	--	--	--	3.84
60 ×3	0.09	0.1	0.53	1.19	1.23	--
60 ×4	0.10	0.2	1.98	2.00	2.68	--
60 ×5	0.12	0.8	7.33	--	--	--
60 ×6	0.35	--	--	--	--	--
60 ×8	1.10	--	--	--	--	--
140 ×1	--	--	--	--	--	3.03
140 ×2	--	--	--	--	--	4.92
140 ×3	0.09	0.2	1.39	1.25	1.69	--
140 ×4	0.14	0.3	5.53	4.08	6.54	--
140 ×5	0.19	1.6	--	--	--	--
140 ×6	0.33	--	--	--	--	--
140 ×8	1.60	--	--	--	--	--

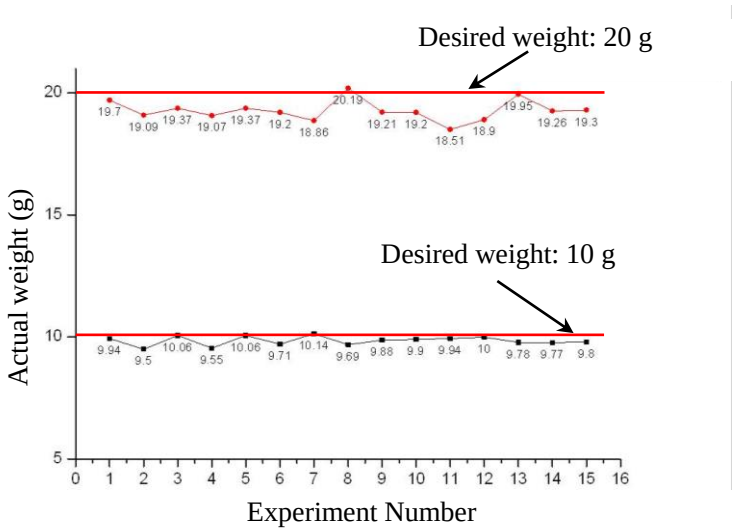

Fig. 7. Errors between the desired and actual weight in powder supplying

3.2. Homogeneity of Powder Mixture

Pure Cu and Ni powders were used to test the powder mixing quality. The two kinds of powders were mixed by the system at a desired proportion, and then the mixture was spread into a layer. Since the color of Cu powder (red) is quite different from that of Ni powder (gray), an image detection method was developed to measure the actual proportion. Micrographs were taken at 10 different locations on the powder layer. The number of red pixels in the micrograph was computed and the proportion of Cu equaled the ratio of the red pixels number to total pixels number.

From the results listed in Table 2, the variation of proportion at different sampling points

is minor and the actual proportion is close to the desired value, showing a good quality of the powder mixing of the system.

Table 2. Proportion of Cu at different sampling points

Sampling point number	Desired value: 0.1	Desired value: 0.3	Desired value: 0.5	Desired value: 0.7	Desired value: 0.9
1	0.0974	0.2981	0.5091	0.6926	0.9233
2	0.1004	0.2873	0.4991	0.7189	0.9105
3	0.0946	0.3089	0.5554	0.7345	0.8987
4	0.0953	0.2854	0.5364	0.7076	0.8952
5	0.0939	0.3070	0.5091	0.6975	0.8961
6	0.0949	0.2843	0.5145	0.7012	0.8957
7	0.0947	0.2865	0.5603	0.7006	0.9043
8	0.0941	0.3037	0.5128	0.6803	0.9022
9	0.0917	0.2868	0.5021	0.7014	0.9126
10	0.0984	0.2968	0.5298	0.7033	0.9039
Average	0.0955	0.2945	0.5229	0.7038	0.9043
Variance	0.0024	0.0091	0.0206	0.0139	0.0085

3.3. Stress on the Spreading Comb Tooth

A finite elements model was established in ANSYS to simulate the stress distribution on a comb tooth which is scarping over a bump. Fig.8 shows the Mises stress distribution on a bended tooth, and the maximum stress appears at the root of the tooth. The maximum Mises stress vs. bump height curves of a comb tooth at various angles were computed and plotted in Fig. 9. The results show that the maximum Mises stress increases with the increase of bump height and decreases with the increase of inclined angle. Compared to a vertical comb, an inclined comb suffers less stress while scarping over a bump with same height. At a bump height of 0.6 mm, the maximum Mises stress of the comb with an inclined angle of 15°is 31.8% of that of vertical comb. A lower stress level means lower risk of breaking for the comb tooth, and thus would efficiently extend the comb lifetime.

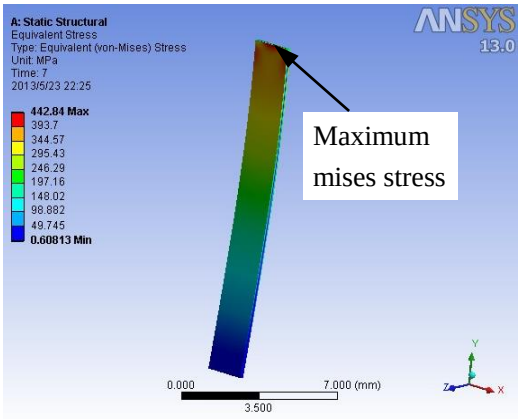

Fig. 8. Mises stress distribution on a bended tooth

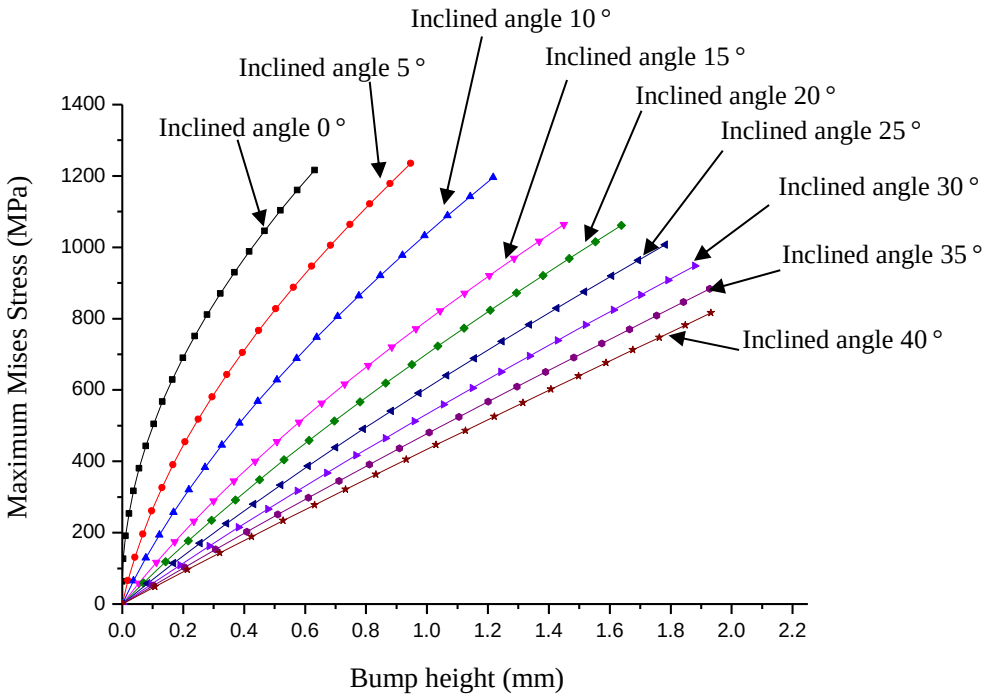

Fig. 9. Maximum Mises stress of the comb tooth scarping over a bump

3.4. Single-Material Processing

Single-material processing was conducted on the EBSM-250 system which adopts the above powder supplier and spreading devices. Materials including 316L stainless steel, Ti-6Al-4V were successfully fabricated. The average relative density of fabricated samples reaches up to 99.96%. The ultimate tensile strength of Ti-6Al-4V sample was 923~1174 MPa, comparable to that of wrought parts. Some Ti-6Al-4V parts fabricated by EBSM are showed in Fig. 10.

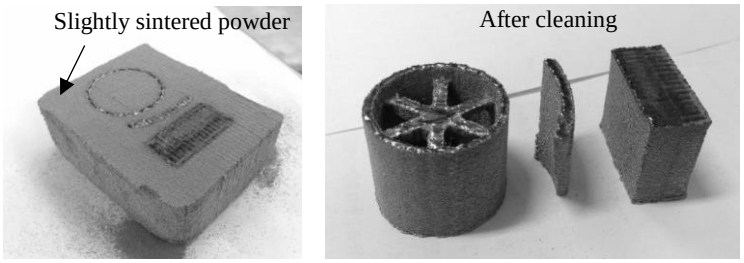

Fig. 10. Ti-6Al-4V parts fabricated by EBSM

3.5. Dual-Materials Processing

A Ti-6Al-4V and TiAl dual-material structure is proposed and planned to be fabricated on the system developed in this paper. Ti-6Al-4V has excellent strength and plasticity at room temperature, while TiAl alloy has excellent performance at high temperature, yet very brittle. Part with Ti-6Al-4V at the cold end, TiAl at the hot end, and graded material at the middle may have potential application prospect. As illustrated in Fig. 11, at the bottom layers material with 100% Ti-6Al-4V and 0% TiAl is deposited. Then the proportion of TiAl increases from 0% to 100% layer by layer, finally turning into 100% TiAl at the top layers. This structure with

dual-performance can be used to build the TiAl impeller with a Ti-6Al-4V rabbet. Compared with the welding interface, the graded material transition would be more controllable and programmable.

However, the dual-materials processing brings challenges to the powder recycle. As the graded parts are fabricated in a single machine run, the two powders are mixed in the building tanks. As a result, the un-used powder is difficult to be recycled and is sacrificed to obtain the graded material.

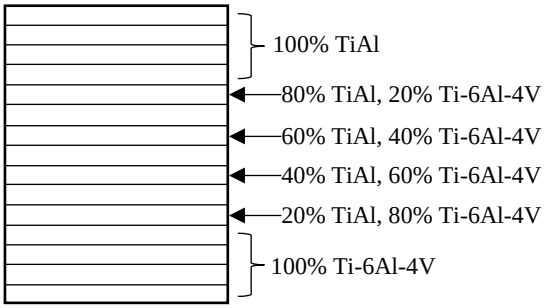

Fig. 11. Ti-6Al-4V and TiAl dual-material structure

Conclusions

1. The vibration driven powder supplier developed in this study has a high compatibility to various powders. A stable supplying rate and a supplying accuracy less than 7.5% were obtained with the supplier.

2. Two powders can be supplied individually to obtain a mixture with tailored proportion. Experimental results show that the mixture is homogenous and the actual proportion is close to the desired value.

3. The powder spreading device based on dual inclined combs can significantly reduce the stress of comb tooth while scraping over a bump and thus has longer lifetime.

4. The EBSM system provides two exchangeable building tanks with sizes of $100 \times 100 \times 100$ mm^3 and $250 \times 250 \times 250$ mm^3.

5. The novel EBSM system is capable of building parts with single material and has a potential of dual-material processing.

Acknowledgements

The authors would like to acknowledge the funding of 2013 Beijing Science and Technology Development Project, No. D13110400300000 and D131100003013002.

References

1. Cormier, D., Harrysson, O. L. A., Mahale, T., West II, H. A., 2008, “Freeform Fabrication of Titanium Aluminide via Electron Beam Melting Using Prealloyed and Blended Powders”, Advanced Material Science and Engineering, 2007, pp. 6822-6825.
2. Facchini, L., Magalini, E., Robotti, P., Molinari, A., 2009, “Microstructure and mechanical properties of Ti-6Al-4V produced by electron beam melting of pre-alloyed powders”, Rapid

Prototyping Journal, 15, pp. 171-178.
3. Murr, L. E., Martinez, E., Pan, X. M., Gaytan, S. M., Castro, J. A., Terrazas, C. A., Medina, F., Wicker, R. B., Abbott, D. H., 2013, “Microstructures of Rene 142 nickel-based superalloy fabricated by electron beam melting”, Acta Materialia, 61, pp. 4289-4296.
4. Sun, S. H., Koizumi, Y., Kurosu, S., Li, Y. P., Matsumoto, H., Chiba, A., 2014, “Build direction dependence of microstructure and high-temperature tensile property of Co-Cr-Mo alloy fabricated by electron beam melting”, Acta Materialia, 64, pp. 154–168.
5. Yan, Y. N., Qi, H. B., Lin, F., He, W., Zhang, H. R., Zhang, R. J., 2007, “Produced three-dimensional metal parts by electron beam selective melting”, Chinese Journal Mechanical Engineering, 43, pp. 87-92.
6. Liu, Z. H., Zhang, D. Q., Sing, S. L., Chua, C. K., and Loh, L. E., 2014, “Interfacial Characterization of SLM Parts in Multi-material Processing: Metallurgical Diffusion between 316L Stainless Steel and C18400 Copper Alloy”, Materials Characterization, 94, pp. 116-125.
7. Terrazas, C. A., Gaytan, S. M., Rodriguez, E., Espalin, D., Murr, L. E., Medina, F., and Wicker, R. B., 2013, “Multi-material metallic structure fabrication using electron beam melting”, International Journal of Advanced Manufacturing Technology, 71, pp. 33-45.